Kang *et al. Geosci. Lett.* (2020) 7:7
https://doi.org/10.1186/s40562-020-00156-6

Geoscience Letters

RESEARCH LETTER

Open Access

On the cloud radiative effect for tropical high clouds overlying low clouds

Hyoji Kang, Yong-Sang Choi*, Jiwon Hwang and Hye-Sil Kim

Abstract

Since high and low clouds ubiquitously overlie the Tropical Western Pacific (TWP) region, the cloud radiative effect (CRE) cannot be influenced by either high or low clouds, but by combinations of the clouds. This study investigates the CRE of multi-layered clouds in TWP via a radiative transfer model, Streamer. We assumed that multi-layered clouds are composed of full coverage of high clouds overlying low clouds with fractional coverage. The simulation results show that low clouds readily change CREs from positive to negative in the case of optically thin high clouds, even if the fraction of low clouds takes 10% of that of high clouds. Also, various combinations of physical properties of multi-layered high and low clouds allow more CRE variability (− 253.76 to 93.10 W m^{-2}) than single-layered clouds do (− 101.62 to 96.95 W m^{-2}). Even in the same conditions (total column cloud optical thickness = 15 and high cloud top pressure = 200 hPa), the multi-layer clouds have various CREs from − 180.55 to 45.64 W m^{-2}, while the single-layer high clouds − 2.00 W m^{-2}. These findings are also comparable with satellite observations from CERES and CALIPSO. The present study suggests that considerable uncertainty of radiative effects of high clouds over TWP can attribute to low clouds below high clouds.

Introduction

Over the Tropical Western Pacific (TWP), high clouds (i.e., cirrus, cirrostratus, and deep convective clouds; Rossow and Schiffer, 1991) have consistently been proposed as primary modulators of the regional climate system's radiation balance due to persistent occurrence and large areal coverage in response to the higher sea surface temperature (SST) (Liou, 1986; Bony et al. 1997; Lynch et al. 2002; Lee et al. 2009). The quantitative contribution of clouds to the radiation balance is called the cloud radiative effect (CRE) relative to the clear sky.

Several studies have reported a wide range of cloud optical thicknesses (COTs) (that determine CREs, accordingly) for high clouds. Choi and Ho (2006) have divided the amount of high clouds into six COT categories from less than 1 to over 60. Kubar et al. (2007) have also categorized high clouds over TWP as thin, anvil, and thick based on their optical thickness from 0 to 64. In addition, Lai et al. (2019) have revealed that COT retrievals of high clouds from three different satellites (Himawari-8, FengYun-4A, and Aqua) commonly range from 0 to 40. Below high clouds, congestus and convective clouds frequently form in shallow-to-deep convective transitions over TWP (Burleyson et al. 2015; Neggers et al. 2007). These studies suggest the COTs may not be entirely due to variations in microphysical properties of high clouds themselves, but more likely due to frequently underlying low clouds below high clouds. Therefore, to understand the CRE over TWP more profoundly, it may be necessary to infer the potential existence of low clouds where high clouds are detected—i.e., multi-layered clouds (Choi and Ho 2006).

These multi-layered clouds may not be well-reflected in current satellite observations because most meteorological satellites generally have visible/infrared sensors that are not able to penetrate the atmosphere vertically. Thus, the satellites produce cloud information under the assumption of single-layered clouds. For this reason, previous studies about CREs using satellite retrievals may

*Correspondence: ysc@ewha.ac.kr
Department of Climate and Energy Systems Engineering, Ewha Womans University, EngineerB 353, 52 Ewhayeodae-gil, Seodaemun-gu, Seoul 03760, South Korea

include significant uncertainties because of not knowing whether the high clouds are single- or multi-layered (Mace et al. 2009; L'Ecuyer et al. 2019). Note that only a few satellites such as Cloudsat and CALIPSO have measured the vertical information of clouds since 2006 (Im et al. 2005; Winker et al. 2007); the narrow field-of-view of their active radar and lidar sensors is insufficient to capture the fractional change of clouds by the layer.

High clouds composed of relatively large ice particles tend to reflect small amounts of shortwave (SW) radiation. In contrast, their contribution to outgoing longwave (LW) radiation is weak due to their far lower cloud top temperature relative to the SST, thus leading to a positive (i.e., warming) CRE. However, it remains uncertain as underlying low clouds add COT to that of high clouds (Choi and Ho 2006); high clouds pretend to have various CREs in response to their COTs. On the one hand, low clouds, including cumulus, stratocumulus, and stratus (Rossow and Schiffer 1991), have a robust negative CRE due to their considerable COTs with smaller and more compact liquid particles and also relatively higher cloud top temperature. In the case of multi-layered clouds, interactive radiative effects between high and low clouds in different layers might also influence the CRE, in addition to the variability in each high and low clouds.

Despite these potentials, the question of how multi-layered clouds contribute to the top-of-atmosphere (TOA) radiative balance has yet to be examined. The present study, therefore, aims at investigating the CRE of high clouds overlying low clouds using a radiative transfer model. Due to limitations of current satellites for detecting daily fractional changes of multi-layered clouds (Kim et al. 2011; L'Ecuyer et al. 2019), the present study simulated high clouds overlying low clouds by varying COT, cloud top pressure (CTP) and cloud fraction (CF). CRE ranges from simulations were then compared with those observed by satellites using daily TOA radiative fluxes from the CERES instruments on satellite Aqua, along with cloud properties derived from the MODIS and CALIOP.

Data and method

The CRE is the difference in the TOA radiative flux between all-sky (including diverse clouds) and clear-sky conditions. The contribution of a cloud to the reflection of SW radiation is the SW CRE:

$$\text{SW CRE} = S\left(\alpha_{\text{clear}-\text{sky}} - \alpha_{\text{all}-\text{sky}}\right) \quad (1)$$

where S is the solar insolation; $\alpha_{\text{clear-sky}}$ and $\alpha_{\text{all-sky}}$ are the albedo in clear-sky and all-sky conditions, respectively.

On the other hand, clouds trap LW radiation emitted from below and re-emit a proportion of this to space depending on cloud top temperature. The contribution of a cloud to LW radiation is the LW CRE, the difference in the upward LW flux between all-sky ($F_{\text{all-sky}}$) and clear-sky ($F_{\text{clear-sky}}$) conditions:

$$\text{LW CRE} = F_{\text{clear}-\text{sky}} - F_{\text{all}-\text{sky}}. \quad (2)$$

By Eqs. (1) and (2), SW CRE is negative, while LW CRE is positive. A positive CRE represents a warming effect on the Earth, whereas a negative CRE indicates a cooling effect. Finally, the net CRE can then be calculated by the summation of the SW CRE and LW CRE.

We used a radiative transfer model Streamer since the model allows the flexible specification of physical properties such as the presence of multi-layered clouds and user-specified optical properties (Key, 1999). For simplicity, the present study assumed that multi-layered clouds have a full coverage of high clouds ($\text{CF}_{\text{high}} = 1.0$) and the varying fraction of low clouds ($\text{CF}_{\text{low}} = 0.1$, 0.5, and 1.0) (Fig. 1). Simulations are conducted using plane-parallel clouds with input parameters summarized in Table 1. In the present model, the CRE at the TOA is modulated not only by optical properties (CTPs and COTs) of high and low clouds, but also by the CF_{low}; $\text{CF}_{\text{low}} < 1$ means that high clouds partly overlie low clouds. High clouds and low clouds are simulated with varying CTPs, 100, 200, and 300 hPa and 600, 700, and 800 hPa, respectively. COTs are set to be 0.5–25 for high clouds and 5–35 for low clouds (Lai et al. 2019). The COT ranges are appropriate for the examination of a variety of multi-layered clouds composed of optically distinct high and low clouds over TWP (L'Ecuyer et al. 2019; Kubar et al. 2007). According to previous studies (Yi et al. 2017; Key, 1999), the effective radius of high and low clouds is fixed as their typical values of 30 and 13 μm, and the water content as 0.06 and 0.30 g m^{-3}, respectively.

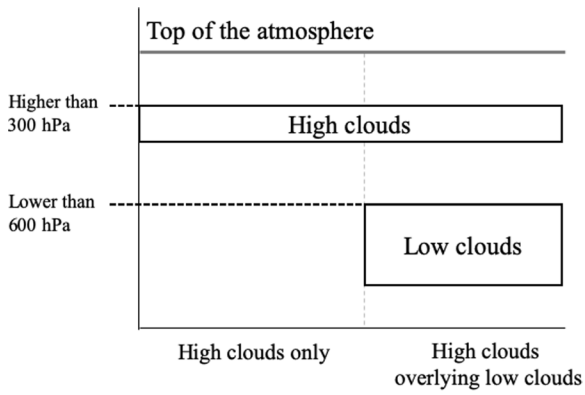

Fig. 1 A schematic diagram of high clouds overlying low clouds over the Tropical Western Pacific region. Here, high and low clouds are defined as by $\text{CTP}_{\text{high}} \leq 300$ hPa and $\text{CTP}_{\text{low}} \geq 600$ hPa, respectively

Table 1 Details of the input parameters for radiative transfer model simulations

Cloud properties	Input parameters
Cloud fraction	
High	1*
Low	0.1, 0.5, 1.0
Cloud top pressure [hPa]	
High	100, 200, 300
Low	600, 700, 800
Effective radius [μm]	
High	30*
Low	13*
Water content [g m^{-3}]	
High	0.06*
Low	0.3*
Cloud optical thickness	
High	0.5, 1, 3, 5, 7, 9, 15, 20, 25
Low	5, 10, 15, 20, 25, 30, 35
Cloud particle thermodynamic phase	
High	Spherical*
Low	Liquid*

The fixed input parameters are marked with an asterisk

For a fair comparison with the observed CREs, the simulated CREs are corrected by adjusting the S in Eq. (1) to the observed monthly averages of incoming solar flux and the $F_{\text{clear-sky}}$ in Eq. (2) to the observed monthly averages of clear-sky flux, both of which are obtained from the dataset of CERES Energy Balanced and Filled (EBAF)-TOA Edition 4.1 data product (Loeb et al. 2018).

Satellite-observed CREs are calculated for each grid box over TWP (10°N-10°S, 130°E-170°W) according to Eqs. (1) and (2). Different datasets are used for each $F_{\text{all-sky}}$ and $F_{\text{clear-sky}}$ in the calculation of CREs for a month of August 2015. The $F_{\text{all-sky}}$ is the daily averaged value from the CERES Single Scanner Footprint TOA/Surface Fluxes and Clouds One Degree (SSF1deg) Day Edition 4A product (Minnis et al. 2011; Loeb et al. 2018), while the $F_{\text{clear-sky}}$ is the monthly averaged value from the CERES EBAF data. The CERES SSF1deg data provide instantaneously scanned radiative fluxes and thus include the large quantity of clear-sky fluxes as missing values. Thus, the CERES EBAF data spatially interpolate clear-sky fluxes and provide clear-sky fluxes for both cloud-free and cloudy portions. Since clouds cover most of areas in TWP, the CERES EBAF data are used instead of the CERES SSF1deg data for the clear-sky condition to obtain sufficient $F_{\text{clear-sky}}$.

The CREs calculated from the CERES data are classified by cloud height, degree of opacity, and cloud layers. For cloud height and opacity, we used CTP and daytime COT from CERES SSF1deg data that are generated by combining the instantaneous CERES data (20 km × 20 km) with the cloud products from MODIS (1 km × 1 km). The cloud layers are from the CALIPSO Lidar Level 2 5 km cloud layer data version 4.20, which provide high-resolution vertical profiles of clouds (Hunt et al. 2009). We regenerate cloud layer data from CALIPSO to match the spatial resolution to that of CERES. A single- (multi-) layered cloud grid is selected when the detection of single-layered clouds occupies more (less) than 80% within a grid of CERES.

Results

The simulated CREs of multi-layered clouds are presented in Fig. 2, for different CTP of high clouds (CTP_{high}) (the row) and CF_{low} (the column). In each graph, COT of low clouds (COT_{low}) is in the *x*-axis, and COT of high clouds (COT_{high}) is in the *y*-axis. Here, CTP of low clouds (CTP_{low}) is fixed at 700 hPa, because the change in CTP_{low} seldom affects CRE. Note that CF_{high} is unity in all the simulated cases.

Figure 2a (CTP_{high} = 100 hPa and CF_{low} = 0.1) shows strong positive CREs in most cases except for $COT_{high} < 1$. This is because LW CRE of high clouds is predominant over that of low clouds (CF_{high} = 1 vs. CF_{low} = 0.1). However, when high clouds become optically very thin ($COT_{high} < 1$, solid contour), CRE turns out to be negative. This implies that even small CF_{low} can be significant for enhancing negative CREs under the presence of optically very thin high clouds. In such cases of CF_{low} = 0.1 (Fig. 2a, d, g), CRE is mainly altered by COT_{high} rather than COT_{low}.

The influence of CF_{low} upon CREs can be elucidated by comparing Fig. 2a (CF_{low} = 0.1), Fig. 2b (CF_{low} = 0.5) and Fig. 2c (CF_{low} = 1.0) (all cases are for CTP_{high} = 100 hPa). Radiative effects of low clouds become stronger, in response to increased CF_{low}. The role of low clouds in controlling the CRE is maximized when CF_{low} = 1.0. A decrease in the CRE of multi-layered clouds with increasing COT_{low} is more significant for larger CF_{low}. Regardless of CTP_{high}, CRE is subject to COT_{low} for large CF_{low}, while it is not true for small CF_{low} (compare Fig. 2d–f or compare Fig. 2g–i). The possible range of CRE is broaden for larger CF_{low}: − 113.76 to 93.02 W m^{-2} for CF_{low} = 0.1, − 162.33 to 77.26 W m^{-2} for CF_{low} = 0.5, and − 223.06 to 57.55 W m^{-2} for CF_{low} = 1.0.

As CTP_{high} decreases, the LW trapping effect of high clouds is weakened. As a result, CREs become negative. The possible range of CRE in case of CTP_{high} = 100 hPa (300 hPa) is from − 187.99 to 93.01 W m^{-2} (from − 223.03 to − 4.26 W m^{-2}).

Throughout Fig. 2, CREs for COT_{high} = 5 are particularly notable since they are showing maximum CREs

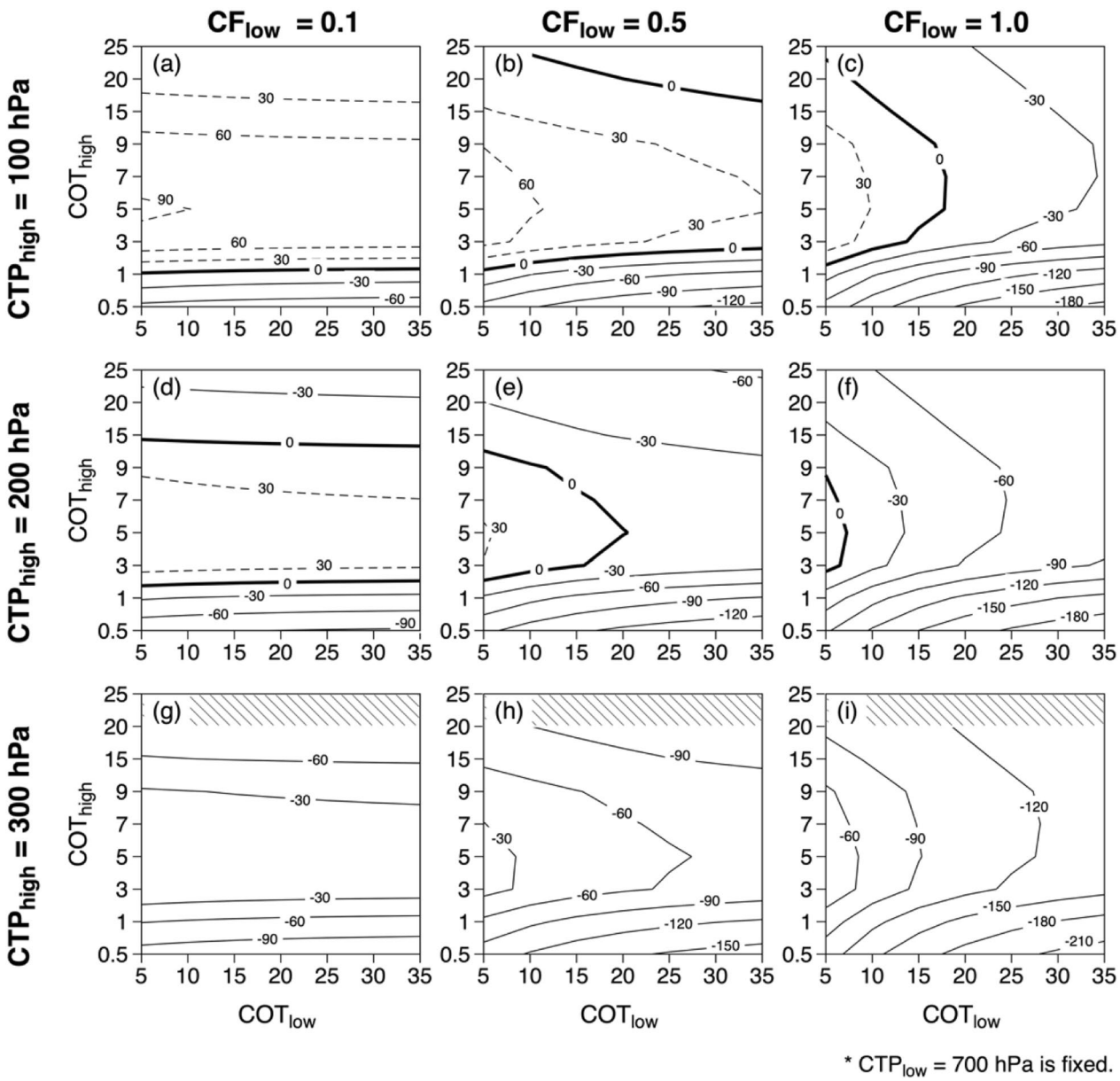

Fig. 2 Contour graphs for CREs of multi-layered clouds simulated from a radiative transfer model Streamer. Columns (left to right) indicate increase in CF_{low} as 0.1, 0.5 and 1.0, while rows represent various levels of high clouds. Note that CTP_{low} is fixed as 700 hPa since the impact of any change in CTP_{low} upon radiative effect is negligible in multi-layered clouds. *x*- and *y*-axes represent diverse COT_{low} and COT_{high}, respectively. Contour lines are CREs which are drawn at intervals of 30 W m^{-2}. Dashed and solid lines represent positive and negative CREs, respectively; the zero-reference line is shown as thick line. Shaded areas on the bottom row indicate missing values due to overlap of cloud thicknesses between high and low clouds

in each graph. This finding implies $COT_{high} = 5$ is thin enough for SW flux to penetrate (the smallest SW CRE) but, at the same time, thick sufficient for LW flux to be trapped (the largest LW CRE). When $COT_{high} < 5$, low clouds are dominant to the determination of CREs, while $COT_{high} > 5$, relatively thick high clouds contribute more by reflecting SW and trapping LW radiations. Note that we used the observed monthly averages of incoming solar flux in the calculation of SW CRE. Therefore, the monthly average-based CRE in Fig. 2 is subjective to the insolation depending on time and region. For example, the decrease in insolation due to increase in the solar zenith angle may weaken the SW CRE.

Now, Fig. 3 compared the multi-layered clouds with the single-layered clouds for $3 \leq COT < 9$ (thin lines) and $9 \leq COT < 25$ (thick lines). The criteria of COT for

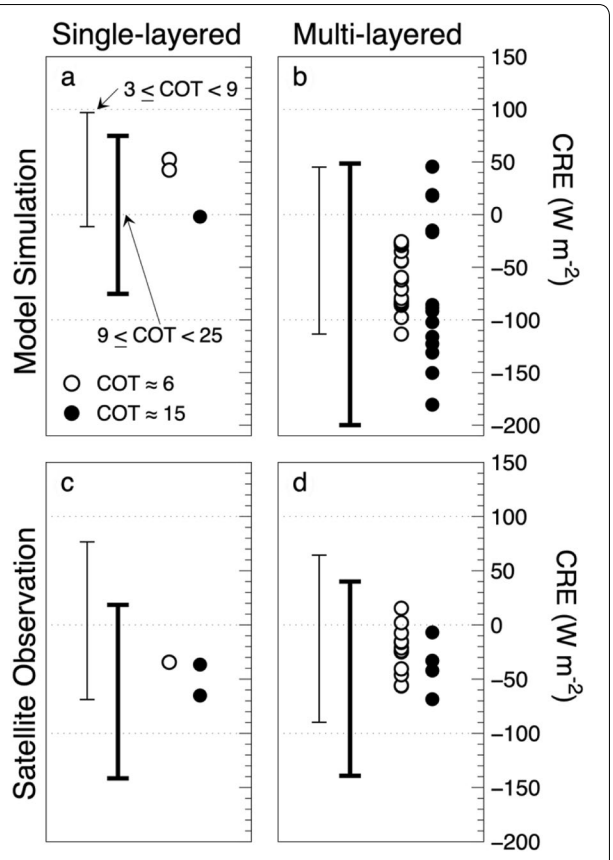

Fig. 3 Comparison of CREs between model simulations (**a**, **b**) and satellite observations (**c**, **d**). Left and right plots in each row represent single-layered clouds (**a**, **c**) and multi-layered clouds (**b**, **d**). Thin and thick lines show full CRE ranges for each $3 \leq \mathrm{COT} < 9$ and $9 \leq \mathrm{COT} < 25$, respectively. Hollow and filled circles each indicate CREs when COT is constrained at 6 and 15, for the limited $\mathrm{CTP}_{\mathrm{high}}$ of 200 to 270 hPa

thin and thick clouds in this figure refer to the International Satellite Cloud Climatology Project (ISCCP) cloud type classification (Rossow and Schiffer 1991). In addition, the hollow and filled circles in Fig. 3 represent the CREs for specific cases constrained by COT of 6 and 15, respectively. Here, COT is the summation of $\mathrm{COT}_{\mathrm{high}}$ and $\mathrm{COT}_{\mathrm{low}}$, to compare with the satellite-retrieved COT.

In the simulations, combinations of microphysical and macrophysical properties of high and low clouds may induce a broader range of CREs. For thin clouds ($3 \leq \mathrm{COT} < 9$), single-layered clouds show a variation in CREs from −11.39 to 96.95 W m^{-2}, whereas multi-layered clouds from −113.40 to 45.12 W m^{-2} (thin lines in Fig. 3a vs. b). Likewise, for thick clouds ($9 \leq \mathrm{COT} < 25$), a CRE range of multi-layered clouds become broader (from −199.93 to 48.54 W m^{-2}) than those of single-layered clouds (from −75.31 to 74.82 W m^{-2}) (thick lines in Fig. 3a vs. b). These features are apparent even when COT is a specific value. For $\mathrm{COT} = 6$ (hollow circles), corresponding single-layered clouds (Fig. 3a) show CREs from 42.30 to 52.40 W m^{-2}, while multi-layered clouds (Fig. 3b) show a broader variation in CREs from −113.40 to −25.60 W m^{-2}. For $\mathrm{COT} = 15$ (filled circles), the CRE of single-layered clouds (Fig. 3a) is −2.00 W m^{-2}, while multi-layered clouds (Fig. 3b) have a more extensive range of CREs (from −180.55 to 45.64 W m^{-2}). This distinct difference suggests that, even in the same conditions for CTP and COT, combinations of high and low clouds produce a broader range of CREs than single-layered clouds do.

To validate the simulated CREs of multi-layered clouds discussed above, we superimposed the satellite-observed CREs with the identical constraints of COT and CTP to the simulated CREs (Figs. 3c, d) except for $\mathrm{CTP}_{\mathrm{high}}$. Due to a lack of samples with $\mathrm{CTP}_{\mathrm{high}} = 200$ hPa, we had to allow samples with $\mathrm{CTP}_{\mathrm{high}}$ from 200 to 270 hPa from the satellite observations. Nevertheless, the ranges of CREs in satellite observations were comparable with those in the simulations.

Like the simulations, a wide variety of CREs of multi-layered clouds are also found in the observations. For $\mathrm{COT} = 6$ (hollow circles), single-layered clouds (Fig. 3c) have CRE = −34.39 W m^{-2}, while multi-layered clouds (Fig. 3d) have a more extensive CRE range (from −56.25 to 15.51 W m^{-2}). For $\mathrm{COT} = 15$ (filled circles), single-layered clouds have narrower CREs (from −65.11 to −36.57 W m^{-2}) than multi-layered clouds do (from −68.54 to −6.90 W m^{-2}).

Finally, the observational range in CREs between single-layered and multi-layered clouds is not as different as the simulated range for $3 \leq \mathrm{COT} < 9$ (thin lines) or $9 \leq \mathrm{COT} < 25$ (thick lines) in Fig. 3c, d. For $3 \leq \mathrm{COT} < 9$ ($9 \leq \mathrm{COT} < 25$), the single-layered clouds range from −68.82 to 76.66 W m^{-2} (−141.53 to 18.51 W m^{-2}), and the multi-layered clouds range from −89.80 to 64.38 W m^{-2} (−139.15 to 40.05 W m^{-2}). This may be attributable to insufficient observational constraints corresponding to the simulated conditions ($\mathrm{CTP}_{\mathrm{high}}$, $\mathrm{CF}_{\mathrm{high}}$, $F_{\mathrm{clear\text{-}sky}}$, etc.) that will be discussed in the next section.

Summary and discussions

The present study has demonstrated that multi-layered clouds show more extensive variations in CREs compared to single-layered clouds from a radiative transfer model Streamer. Here, we summarize how different conditions in multi-layered clouds alter CREs. First, low clouds play a crucial role in controlling CREs. As $\mathrm{CF}_{\mathrm{low}}$ becomes larger, CREs will get more negative. Low clouds can change CREs from positive to negative when high clouds are optically thin, even if $\mathrm{CF}_{\mathrm{low}}$ takes only 10% of $\mathrm{CF}_{\mathrm{high}}$. Regardless of the combinations, it is intriguing that the cases for $\mathrm{COT}_{\mathrm{high}} = 5$ show maximized CREs of

multi-layered clouds. Another interesting aspect is that multi-layered clouds induce large CRE variations, even though the top pressure of high clouds and the total column COT are in the same conditions. The top pressure and the total column COT are being consistently retrieved from satellites.

Nevertheless, there still remain several limitations and further questions in this study. First of all, the estimation on the precise CREs and on microphysical properties of both single- and multi-layered clouds is rendered difficult due to extensive spatial resolution of CERES sensor. Therefore, mixed effects of single- and multi-layered clouds and indistinct cloud properties could remain in the results from satellite observations. Second, there might be an uncertainty in CRE resulted from the dependence on insolation. If daily mean insolation is adjusted instead of monthly mean, the results could reflect more detailed CRE ranges. Third, the response of multi-layered clouds to other variables, such as SST, should be further investigated. Any changes in microphysical or macrophysical cloud properties in response to SST could significantly affect the structure of multi-layered clouds, and hence, their contributions to the radiative balance. Therefore, investigation on this relationship would be helpful to clearly delineate the participation of multi-layered clouds in climate feedback processes over TWP. Last, we suggest satellite algorithms estimating CREs to be more careful on their simplified assumption about the cloud layer using a radiative transfer model. Since those algorithms provide CREs of multi-layered clouds as those from single-layered clouds, interpretation on CREs will be misled. Such misleading will inhibit precise understanding on CREs over TWP.

However, beyond such limitations, this study highlights the importance of considering the potential variability of multi-layered clouds when interpreting their influence on the energy balance of the climate system.

Acknowledgements
This research was supported by Basic Science Research Program through the National Research Foundation of Korea (NRF) funded by the Ministry of Education (2018R1A6A1A08025520).

Authors' contributions
HJK performed the model simulation and data analysis and wrote the major section of the paper. YSC provided the issue of multi-layered cloud structure shown in this study and guidance of this study. JWH contributed to prepare satellite observation dataset and review the manuscript. HSK supervised the thorough model simulation and interpretation on the results. All authors read and approved the final manuscript.

Availability of data and materials
The data and materials analyzed in this study are accessible from the corresponding author under reasonable request.

Competing interests
The authors declare that they have no competing interests.

Received: 15 December 2019 Accepted: 25 May 2020
Published online: 29 May 2020

References

Bony S, Lau KM, Sud YC (1997) Sea surface temperature and large-scale circulation influences on tropical greenhouse effect and cloud radiative forcing. J Clim 10(8):2055–2077
Burleyson CD, Long CN, Comstock JM (2015) Quantifying diurnal cloud radiative effects by cloud type in the tropical western Pacific. J Appl Meteorol Climatol 54(6):1297–1312
Choi YS, Ho CH (2006) Radiative effect of cirrus with different optical properties over the tropics in MODIS and CERES observations. Geophys Res Lett. https://doi.org/10.1029/2006GL027403
Hunt WH, Winker DM, Vaughan MA, Powell KA, Lucker PL, Weimer C (2009) CALIPSO lidar description and performance assessment. J Atmos Ocean Technol 26(7):1214–1228
Im E, Durden SL, Wu C (2005) Cloud profiling radar for the Cloudsat mission. IEEE Trans Aerosp Electron Syst. 20:15–18
Key JR (1999) Streamer user's guide. Technical report
Kim SW, Chung ES, Yoon SC, Sohn BJ, Sugimoto N (2011) Intercomparisons of cloud-top and cloud-base heights from ground-based Lidar, CloudSat and CALIPSO measurements. Int J Remote Sens 32(4):1179–1197
Kubar TL, Hartmann DL, Wood R (2007) Radiative and convective driving of tropical high clouds. J Clim 20(22):5510–5526
L'Ecuyer TS, Hang Y, Matus AV, Wang Z (2019) Reassessing the effect of cloud type on Earth's energy balance in the age of active spaceborne observations. Part I: top of atmosphere and surface. J Clim 32(19):6197–6217
Lai R et al (2019) Comparison of cloud properties from Himawari-8 and FengYun-4A Geostationary Satellite Radiometers with MODIS Cloud Retrievals. Remote Sensing 11(14):1703
Lee J, Yang P, Dessler AE, Gao BC, Platnick S (2009) Distribution and radiative forcing of tropical thin cirrus clouds. J Atmos Sci 66(12):3721–3731
Liou KN (1986) Influence of cirrus clouds on weather and climate processes: a global perspective. Mon Weather Rev 114(6):1167–1199
Loeb NG, Doelling DR, Wang H, Su W, Nguyen C, Corbett JG, Liang L, Mitrescu C, Rose FG, Kato S (2018) Clouds and the earth's radiant energy system (CERES) energy balanced and filled (EBAF) top-of-atmosphere (TOA) edition-4.0 data product. J Clim 31(2):895–918
Lynch DK, Sassen K, Starr DOC, Stephens G (eds) (2002) Cirrus. Oxford University Press, Oxford
Mace GG, Zhang Q, Vaughan M, Marchand R, Stephens G, Trepte C, Winker D (2009) A description of hydrometeor layer occurrence statistics derived from the first year of merged Cloudsat and CALIPSO data. J Geophys Res Atmos. https://doi.org/10.1029/2007JD009755
Minnis P, Sun-Mack S, Young DF, Heck PW, Garber DP, Chen Y, Spangenberg DA, Arduini RF, Trepte QZ, Smith WL, Ayers JK (2011) CERES Edition-2 cloud property retrievals using TRMM VIRS and Terra and Aqua MODIS data—Part I: algorithms. IEEE Trans Geosci Remote Sens 49(11):4374–4400
Neggers RA, Neelin JD, Stevens B (2007) Impact mechanisms of shallow cumulus convection on tropical climate dynamics. J Clim 20(11):2623–2642
Rossow WB, Schiffer RA (1991) ISCCP cloud data products. Bull Am Meteor Soc. https://doi.org/10.1175/1520-0477(1991)072%3c0002:ICDP%3e2.0.CO;2
Winker DM, Hunt BH, McGill MJ (2007) Initial performance assessment of CALIOP. Geophys Res Lett 34:L19803
Yi B, Rapp AD, Yang P, Baum BA, King MD (2017) A comparison of Aqua MODIS ice and liquid water cloud physical and optical properties between collection 6 and collection 5.1: pixel-to-pixel comparisons. J Geophys Res Atmospheres 122(8):4528–4549

Publisher's Note